Published in final edited form as:
Radiat Res. 2013 October ; 180(4): 398–406. doi:10.1667/RR3363.1.

Thermal Injury Lowers the Threshold for Radiation-Induced Neuroinflammation and Cognitive Dysfunction

Jonathan D. Cherry[a], **Jacqueline P. Williams**[b], **M. Kerry O'Banion**[c], and **John A. Olschowka**[c,1]

[a] Department of Pathology and Laboratory Medicine, University of Rochester School of Medicine and Dentistry, Rochester, New York 14642

[b] Department of Radiation Oncology, University of Rochester School of Medicine and Dentistry, Rochester, New York 14642

[c] Department of Neurobiology & Anatomy, University of Rochester School of Medicine and Dentistry, Rochester, New York 14642

Abstract

The consequences of radiation exposure alone are relatively well understood, but in the wake of events such as the World War II nuclear detonations and accidents such as Chernobyl, other critical factors have emerged that can substantially affect patient outcome. For example, ~70% of radiation victims from Hiroshima and Nagasaki received some sort of additional traumatic injury, the most common being thermal burn. Animal data has shown that the addition of thermal insult to radiation results in increased morbidity and mortality. To explore possible synergism between thermal injury and radiation on brain, C57BL/6J female mice were exposed to either 0 or 5 Gy whole-body gamma irradiation. Irradiation was immediately followed by a 10% total-body surface area full thickness thermal burn. Mice were sacrificed 6 h, 1 week or 6 month post-injury and brains and plasma were harvested for histology, mRNA analysis and cytokine ELISA. Plasma analysis revealed that combined injury synergistically upregulates IL-6 at acute time points. Additionally, at 6 h, combined injury resulted in a greater upregulation of the vascular marker, ICAM-1 and TNF-α mRNA. Enhanced activation of glial cells was also observed by CD68 and Iba1 immunohistochemistry at all time points. Additionally, doublecortin staining at 6 months showed reduced neurogenesis in all injury conditions. Finally, using a novel object recognition test, we observed that only mice with combined injury had significant learning and memory deficits. These results demonstrate that thermal injury lowers the threshold for radiation-induced neuroinflammation and long-term cognitive dysfunction.

INTRODUCTION

Radiation injury is not the only harmful process to consider when modeling a nuclear disaster. Blast injury, blunt trauma and thermal burns have all been observed contribute to morbidity and mortality (1). Typically, these injuries do not occur individually. For example, in past nuclear disasters, such as Hiroshima, Nagasaki and Chernobyl, 60–70% of the radiation-exposed population received a secondary traumatic injury, the most common being thermal burn injury (2). The biology of each injury alone is relatively well understood; however, when these injuries occur in combination, the resulting pathology can be

[1]Address for correspondence: Department of Neurobiology & Anatomy, University of Rochester School of Medicine and Dentistry, Rochester, NY 14642; John_Olschowka@urmc.rochester.edu..

significantly worse. This phenomenon has been termed by some as a “combined injury syndrome” and greatly complicates the pathophysiological mechanism of injury (3). Exploration of synergism between injuries has been conducted in terms of overall survival (4, 5), but data are lacking on how combined injuries affect the central nervous system (CNS) in terms of both pathology and long-term cognitive function.

In the CNS, high doses of radiation have been shown to result in a disruption of the blood brain barrier and activation of glial cells, inducing neuroinflammation (6). However, in a disaster scenario, the majority of survivors will be exposed to relatively low doses of radiation (7), which are not typically associated with inducing observable neuroinflammation (6). Nonetheless, of potential concern is radiation-associated impairment in learning and memory that is observed in the clinical setting, after individuals receive whole brain radiation therapy (8). Decreased cognitive functions have also been suggested as a risk within the low dose space environment (9). These concerns are carried over to nuclear disaster scenarios such as at Chernobyl where those tasked with cleaning up in the aftermath of the disaster performed worse in neurocognitive assessments than those who were not exposed to high radiation levels (10).

Although not commonly associated with affecting the CNS, cognitive alterations have been reported after burn injury (11). Moreover, severe burns compromise the blood brain barrier (12) while less severe, nonlethal burns can alter brain glucose metabolism (13). Burn injury is thought to exert its harmful effect through the robust release of inflammatory agents, such as cytokines and damage associated molecular patterns (DAMPs) from the damaged tissue (14). These released factors can trigger intense systemic inflammation, a condition associated with multiorgan dysfunction syndrome and death (15, 16). We have hypothesized that burn-associated systemic inflammation has the potential to synergize with radiation-induced damage such that low, nonlethal levels of each injury results in enhanced damage compared to either injury alone. In the current study, we demonstrate that a nonlethal 10% total-body surface area (TBSA) thermal burn combined with 5 Gy whole-body γ irradiation leads to enhanced acute systemic and CNS inflammation. In addition, we found that combined injury results in impaired neurogenesis and long-term cognitive dysfunction.

MATERIALS AND METHODS

Animals

Female C57BL/6J mice (n = 128) were purchased from the Jackson Laboratory (Bar Harbor, ME) at 10 weeks of age. The early time points of 6 h and 1 week included six animals per treatment condition. To ensure we had the proper numbers of mice for behavior testing, the 6 month time point included 20 animals per condition. Mice were housed 3–5 per cage in temperature controlled (23 ± 3°C) rooms, with 12-h light/dark cycle and free access to chow and water. Animals were allowed to acclimate for at least 7 days prior to experiments. Animal protocols were reviewed and approved by the University of Rochester Institutional Animal Care and Use Committee.

Combined Radiation-Burn Injury

Our combined injury protocol was based on procedures developed by Kovacs *et al*. (17). Animals were anesthetized intraperitoneally with ketamine (72 mg/kg) and xylazine (5.6 mg/kg) in sterile saline and pretreated subcutaneously with buprenorphine (0.3 mg/kg). Their dorsal surfaces were shaved and any remaining hair was removed with medical depilatory (Nair, Princeton, NJ). Mice were placed on a ^{137}Cs irradiator (J. L. Shepherd & Associates, San Fernando, CA) and exposed to a single dose of 5 Gy. Immediately after irradiation, mice were placed in an enclosed plastic carrier with an opening that exposed

10% of their dorsal surface. Body surface area was determined based on the calculations previously described (18). To reproducibly burn 10% of the dorsal surface, four different carriers were constructed to account for variation in mouse size and weight. Full thickness burn injury was induced by immersing the plastic carrier in a 90°C water bath for 8 s. On the dorsal surface, only areas below the neck and above the hind limbs were exposed to the heated water. Special attention was given to make sure no other areas were exposed. In particular, limbs and the tail were kept inside the carrier to avoid burn injury. A depiction of the approximate area burned is shown in Fig. 1. Animals were removed immediately from the carrier, dried off and injected with 1 ml of lactated Ringer's solution to compensate for any fluid loss.

Tissue and Plasma Collection

Mice were euthanized at 6 h, 1 week or 6 months post-injury. Twenty-four hours prior to euthanasia of the 6 month time point, mice were injected intraperitoneally with 150 mg/kg of BrdU (Sigma-Aldrich, St. Louis, MO). At each time point, animals were fully anesthetized, followed by opening of the thoracic cavity to expose the heart. Using a 27 gauge preheparinized needle, 200–500 μl of blood was drawn from the right ventricle. Blood was subjected to centrifugation at 500*g* at 4°C for 5 min. Plasma was separated and frozen at −80°C for ELISA. After plasma collection, the mice were perfused with saline as previously described (19). The brains were removed and hemisected: one hemisphere was flash frozen in −70°C isopentane for qRT-PCR while the other half was fixed in 4% paraformaldehyde at 4°C overnight and then transferred to 30% sucrose solution overnight or until equilibrated. Upon equilibration, brains were flash frozen in −70°C isopentane and stored at −80°C.

Plasma Cytokine ELISA

Cytokine analysis was performed using IL-6 (KMC0062) and TNF-α (KMC3011) mouse ELISA kits from Invitrogen (Carlsbad, CA). The procedure was conducted according to the manufacturer's protocol. Briefly, 100 μl of plasma was diluted with 100 μl of diluent buffer, added into the provided ELISA plate and incubated for 2 h. A biotinylated antibody conjugate to IL-6 or TNF-α was then added for 30 min. After washing, bound antibody was visualized by a Streptavidin-HRP incubation and reaction. For analysis and calculation of total cytokine levels, an iMark Microplate Absorbance Reader (Bio-Rad, Hercules, CA) was used to measure optical density at 450 nm.

Immunohistochemistry/Immunofluorescence

Brains were sectioned at 30 μm on a sliding microtome with a −25°C stage and stored in cryoprotectant at −20°C. Antibody staining was visualized using biotinylated secondary antibodies, avidin-biotin complex (ABC), and a 3,3 diaminobenzadine (DAB) substrate kit (Vector Laboratories, Burlingame, CA) or, immunofluorescent secondary antibodies bound to Alexa fluorophores 488 or 594 (Invitrogen) at a dilution of 1:500. Primary antibodies used include Armenian Hamster anti-ICAM-1 (1:5,000, Serotec, Kidlington, UK), Rabbit anti-Iba-1 (1:2,000, Wako, Richmond, VA), Rat anti-CD68 (1:2,000, AbD Serotec), Rat anti-CD3 (1:2,000, AbD Serotec), Armenian Hamster anti-CD11c (BD Biosciences, San Jose, CA, 1:500), Rat anti-7/4 (1:3,000, AbD Serotec), Rat anti-MHCII (1:2,000, BD Biosciences), Rat anti-BrdU (1:300, Abcam, Cambridge, UK), and Goat anti-Doublecortin (1:1,000, Santa Cruz Biotechnology, Dallas, TX).

Quantification of Immunohistochemistry

Brain sections were viewed with an Axioplan 2 light microscope (Zeiss, Germany). ICAM-1 and CD68 area was measured at 20× magnification. For ICAM-1, three hippocampal sections per brain were used and multiple images of the cortex were merged together using

Adobe Photoshop CS4. For CD68, two 20× fields per hippocampal section for three different hippocampal slices were used, totaling 6 fields per animal. The images were then subjected to the maximum entropy threshold algorithm in NIH ImageJ (V1.46, http://rsbweb.nih.gov/ij). The percentage of area occupied by ICAM-1 or CD68 was calculated and analyzed. Individual Iba1 cell morphology was visualized using a 63× oil immersion lens. The number of doublecortin positive (DCX+) cells was determined by counting and averaging the total number of DCX+ neurons in the dentate gyrus in 4 sections per animal. The average number of DCX+ cells was then standardized to the average area of dentate gyrus to control for overall area differences. BrdU nalysis was performed by counting total BrdU+ cells that lay directly in the dentate gyrus. Six to seven total hippocampal sections per animal were used, and the average number per section was calculated.

Quantitative Real Time Polymerase Chain Reaction

RNA was isolated from flash frozen half brains using TRIzol (Invitrogen) and an Omni International TH tissue homogenizer according to the manufacturer's protocol. cDNA was prepared using 1 μg of RNA, oligo (dT) and random hexamer primers, and SuperScript III (Invitrogen). qRT-PCR for TNF-α and CCL2 was conducted using predesigned primer/probe sets (Applied Biosystems, Carlsbad, CA). For 18S and ICAM-1, Taqman probe/primer sets constructed with FAM as the fluorescent marker and Blackhole I quencher (Biosearch Technologies, Navato, CA) were used as follows: from 5′ to 3′ 18S, forward primer (F), cct gga tac cgc agc tag gaa, reverse primer (R), act aag aac ggc cat gca cca, and probe (P), cgg cgg cgt tat tcc cat gac c; ICAM1, F, acc atc cca aag ctc gac ac, R, aag aac cac ctt cga ccc act, P, cac tga atg cca gct cgg agg atc ac. Standard curves were generated using serial diluted samples over at least 5 orders of magnitude. PCR reactions were performed using iQsupermix (Bio-Rad) and 1 μl of cDNA. PCR conditions were as follows: denaturation at 95°C for 3 min, followed by 50 cycles of amplification by denaturing at 95°C for 30 s, annealing at 60°C for 30 s and extension at 72°C for 30 s. To determine relative differences in mRNA, reaction efficiency (E) was calculated from a standard curve and cycle threshold (Ct) values were transformed using the equation expression = $(1 + E)^{Ct}$. For normalization, 18S ribosomal RNA was used as the housekeeping gene.

Behavioral Testing

Novel object recognition was used to measure possible effects on memory in mice 6 months after injury. The test was performed and scored as previously described (20). The learning trial time was 10 min and the testing trial time was 5 min. There was a 1-h delay between each trial. In the testing trial, a recognition index (RI) was calculated based on the proportion of time spent with the novel object compared to total time spent with both objects.

Statistics

For statistical analysis, the 6 h, 1 week and 6 month time points were analyzed separately. The only comparison across multiple time points occurred in the controls for CD68 staining to identify an age related increase of baseline. Baselines for all other experiments remained consistent at all time points. To compare the differences between injuries at a single time point a one-way ANOVA was used with a Bonferroni post-test. Only for the ELISA measurements, a Kruskal-Wallis test was used. Statistical computation and graph creation was performed in Graphpad Prism v6 (Graphpad Software, San Diego, CA).

RESULTS

Thermal Injury and Whole-Body Irradiation Result in Systemic Inflammation

The known association between systemic burn-induced inflammation and CNS effects prompted us to first test whether the systemic inflammatory response was enhanced after combined injury. Plasma was isolated at various time points and ELISA was used to measure inflammatory cytokine levels. Analysis of IL-6, which has been implicated in the clinic as a predictor of survival after both burn and traumatic injury (21), revealed significant elevation at 6 h that was limited to plasma from mice with combined injury [Fig. 2A; 1,980 ± 1,269 vs. 0 ± 0 pg/mL in control mice; mean ± SD, ($H = 16.21$, 3 *df*, $P = 0.001$)]. The burn and radiation individual injuries did show some elevation of IL-6; however, the variability was too large to achieve statistical significance. At 1 week, IL-6 levels were reduced, but levels in the combined injury group remained significantly elevated compared to the control mice and the 5 Gy irradiated mice [Fig. 2A; 7.17 ± 4.74 vs. 0 ± 0 and 0 ± 0 pg/mL, respectively, mean ± SD, ($H = 14.93$, 3 *df*, $P = 0.0039$)]. Six months after injury, both the individual burn and the combined injury group had significantly elevated IL-6 levels of 40.2 ± 25.8 and 50.4 ± 37.1 pg/mL, respectively, vs. 2.1 ± 4.5 pg/ml in control mice [mean ± SD ($H = 14.93$, 3 *df*, $P = 0.0019$)]. TNF-α levels did not show significant elevation at any of the selected time points (Fig. 2B).

Injury Leads to Vascular Activation

The vascular endothelium that comprises the blood brain barrier serves to separate the CNS from the periphery. Therefore, brain vasculature sits at a position where it can be affected by both CNS and systemic factors so that neurovascular changes act as a nonspecific indicator of inflammation. Figure 3A shows increases in ICAM-1, a marker of endothelial activation, in the CNS after injury. Using analysis of percentage area covered, we found elevated ICAM-1 staining at 6 h in all three injuries as judged by one-way ANOVA [$F(3,20)=14.72$, $P < 0.0001$] (Fig. 3B). Interestingly, at 1 week, irradiation plus burn injury showed greater ICAM-1 activation relative to either injury alone [$F(3,19) = 14.15$, $P < 0.0001$] (Fig. 3B). Six months after injury, ICAM-1 staining in both the burn and combined injury condition was still significantly elevated [$F(3,35) = 33.61$, $P < 0.0001$)] (Fig. 3B). However the level of staining was not different between the two conditions, suggesting that the long-term effect on ICAM-1 staining was driven mostly by burn injury.

The change in vasculature prompted us to look for infiltration of peripheral immune cells. For the most part, using immunofluorescent analysis, we did not detect any evidence of immune cell infiltration, including CD4+ T cell, CD11c+ dendritic cells, or MHCII+ peripheral macrophage after injury (data not shown). However, we did observe a modest increase in 7/4+ neutrophils 6 h after burn injury. Counts of total neutrophils in 6–7 sections per animal revealed a significant increase of 5 ± 3.6 to 22.7 ± 5.5 or 31.83 ± 12 in the burn and combined injury, respectively, as assessed by a one-way ANOVA [total count ± SD ($F(3,20) = 20.42$, $P < 0.0001$)]. There was no elevation in infiltrating neutrophils with 5 Gy irradiation alone at this time point and no evidence of increased neutrophils at later time points under any condition.

Combined Injury Synergistically Enhances Acute Neuroinflammation

To address whether changes in ICAM-1 staining were associated with evidence of neuroinflammation, we first examined morphology of microglia. In combined injury, at 6 h we observed that many of the microglia had undergone a morphological shift from ramified to a more condensed, activated shape that was not observed with radiation or burn injury alone (Fig. 4A, insets). This type of morphological shift has been associated with glial activation (22). In addition to examining morphology, we used CD68, a lysosomal marker

upregulated in activated microglia. The extent or area of CD68 upregulation has been used to quantify levels of neuroinflammation (23, 24). At 6 h, we observed significantly more CD68 staining in the combined injury group by one-way ANOVA [$F(3,20)$ 5.440, $P = 0.0067$] (Fig. 4B). Increased CD68 staining was also observed with combined injury at 1 week [$F(3,19) = 13.44$, $P < 0.0001$]. Six months after injury, we found an elevation in baseline CD68 staining [$F(2,19) = 72.69$, $P < 0.0001$], which is consistent with reports suggesting age-related increases in microglial activation (25). However, we still observed elevated CD68 staining when comparing the combined injury to the control and burn injury [$F(3,35) = 8.93$, $P = 0.0002$] (Fig. 4B).

To further explore potential synergistic elevations in neuroinflammation, we measured brain mRNA levels of the proinflammatory cytokine TNF-α, which has been associated with neuroinflammation and neurodegenerative diseases (26). At 6 h, we found a significant elevation of TNF-α mRNA in the combined injury when compared to individual injuries by one-way ANOVA [$F(3,18) = 17.08$, $P < 0.0001$] (Fig. 4C). TNF-α levels change significantly at 1 week (Fig. 3C) [$F(3,18) = 3.238$, $P = 0.046$]; however, post hoc analysis did not reveal significant differences between conditions and we did not detect any changes in brain TNF-α mRNA at 6 months.

Thermal Burn and Radiation Injury Result in Impairments in Neurogenesis and Lead to Long-Term Cognitive Dysfunction

Neuroinflammation has been previously shown to alter neurogenesis (27) and impair cognition (28). Using double-cortin (DCX) labeling to identify newly born hippocampal neurons (29), we observed that all three injury groups had significantly reduced numbers of DCX+ cells in the dentate gyrus at 6 months post-injury by one-way ANOVA [$F(3,35) = 58.37$, $P < 0.0001$] (Fig. 5A and B). Similar results were seen when counting BrdU+ cells in the dentate gyrus. Control animals had significantly more BrdU+ cells compared to 5 Gy irradiation, 10% burn, or combined injury (2.7 ± 0.60 vs. 1.1 ± 0.47, 1.8 ± 1.15, or 0.52 ± 0.27, respectively, mean ± SD) [$F(3,35) = 17.52$, $P < 0.0001$)]. To measure long-term changes in learning and memory, a novel object recognition test was employed at this time point. The single burn and radiation injury alone conditions appeared to trend towards a significant decrease compared to the control, however, their mean values never dropped to 50% (Fig. 5C, denoted by the dashed line). Only the combined injury showed significantly worse scores [$F(3,33) = 2.979$, $P = 0.0455$].

DISCUSSION

In earlier reports, we have shown that head-only doses of c radiation greater than 15 Gy are required to induce overt neuroinflammation (6). However, for whole-body exposures occurring as part of a disaster scenario, the majority of survivors of a nuclear incident will be exposed to significantly lower, sub-lethal levels of radiation (30). Since secondary injuries are common in a disaster scenario (2) and when combined with radiation have been shown to result in significantly worse pathology (5). Our aim in this study was to identify evidence for increased neuroinflammation or long-term cognitive impairments that could be manifested after a combined injury of irradiation and thermal burn. Our finding support the contention that multiple injuries can have compounding effects, resulting in worse outcomes than from each injury alone.

The damage induced by burn injury alone is an important factor when considering possible mechanisms by which thermal burn might synergize with radiation-induced injury. In particular, we observed acute elevation of IL-6 expression levels, which is consistent with other reports using this model (17) and which has been reported after irradiation alone (31). Previous studies have shown similar effects of combined injury on other markers of

systemic inflammation, including TNF-α. However, other investigators have shown that TNF-α plasma levels peak at about 90 min post-injury (32) and since our earliest time point was 6 h, we may have missed changes in the level of this cytokine. Other inflammatory factors which have been shown to be upregulated after injury include HMGB1, IL-18, IL-12 and IL-17 (33-36). Like IL-6, any of these factors could be further induced with combined injury. The observed increase in systemic inflammation is very relevant to cognition since peripheral inflammation can lead to short-term, acute behavioral alterations such as sickness behavior (37), as well as long-term cognitive deficits (38, 39). Importantly, many of these studies were carried out in males (17, 32, 36, 41). We used female mice in our experiments and it has been shown that female mice have a less severe response after burn injury compared to males (40). This suggests that the changes we observed could be under representative of the population as a whole. Additional studies with male mice might demonstrate a greater burn-induced CNS effect.

Although radiation or burn injury alone can lead to neuroinflammation, the dose or extent of injury required is typically greater than those used in this study (6, 12). As illustrated in Fig. 3, neither 5 Gy irradiation or 10% thermal burn alone did not result in pronounced neuroinflammation. However, when they occurred in combination, there was a clear increase in glial activation (Fig. 4A and B) and CNS inflammatory cytokine production (Fig. 4C). ICAM-1 expression was also higher when the two injuries occurred together (Fig. 3B). The pathophysiological mechanism of this synergistic elevation is not fully understood, but presumably the systemic inflammation induced by burn injury was enhanced by radiation. Our data do not support an alternate hypothesis that neuroinflammation is dependent upon peripheral cell infiltration. In particular, we did not observe increased numbers of T cells, dendritic cells or macrophages, and the small increase in neutrophils observed at 6 h is not likely to be biologically relevant at the later time points. It is possible that cell infiltration might occur at other time points, but our previous studies of neuroinflammation after irradiation do not reveal clear evidence of peripheral cell infiltration until one month after injury and with doses of 15 Gy| and higher (6).

Even though the mechanism is not clear, neuroinflammation does have links to learning and memory impairments (28) and inhibition of hippocampal neurogenesis (27). In the current study, we found that all injuries led to reductions in hippocampal neurogenesis, as measured by DCX labeling at 6 months. Interestingly, this is one of the first reports to show that burn injury can directly inhibit neurogenesis. This reduction is not surprising given that other systemic inflammatory insults have been reported to induce similar effects (42). Furthermore, systemic factors contribute to reduced neurogenesis associated with aging (43).

To determine if decreased neurogenesis during injury might be associated with cognitive impairment, we used a novel object recognition test. To measure hippocampal dependent memory, we chose to use a delay time of 1 h between the training and trial phase. Using novel object recognition with this time delay has been shown to test mainly the hippocampus, contrary to shorter delays, such as 15 min, which depends on other brain regions (44, 45). Interestingly, only combined injury caused significant reduction in the ability of mice to perform this task. There was a trend for decreased performance with each individual injury (Fig 5C); however, these data were not significant by post hoc analysis. One challenge of the novel object recognition task is the relatively modest difference between successful retention of object recognition and loss of object recognition. It is therefore possible that deficits may have become more apparent with each individual injury if testing had been delayed to a later point after injury. Indeed, in other experiments using doses as low as 3 Gy whole-body irradiation, we have observed reduced performance in novel object recognition 12 months after injury (data not shown). The observation of

reduced cognitive performance with combined injury at this earlier time point (6 months) is therefore consistent with burn injury lowering the threshold for radiation to cause cognitive changes.

In conclusion, we have shown that a 10% TSBA thermal burn and 5 Gy γ irradiation separately do not induce significant neuroinflammation. However, when these injuries occur in combination, there is an increase in acute systemic inflammation as well as CNS inflammation. This synergistic effect also extends to long-term deficits in novel object recognition. The increased inflammation and its known association with cognitive dysfunction (28) suggest potential therapeutic approaches to mitigate such impairments. In particular, in the early aftermath of radiation exposure where there is significant inflammation, the use of anti-inflammatory or anti-immune activation drugs could be a promising treatment strategy. Candidate anti-inflammatory drugs such as minocycline are already FDA-approved and some are currently in clinical trials to treat neurodegenerative diseases where inflammation is prominent (46, 47). Future experiments will be needed to examine the efficacy of these drugs after combined injury and their ability to prevent long-term memory impairment.

Acknowledgments

The authors thank Jack Walter, Lee Trojanczyk, Mallory Olschowka and Sage Begolly for their assistance during mouse irradiations, thermal injury, animal management and tissue processing. We thank Katherine Bachmann in the University of Rochester Environmental Health Sciences Center Behavioral Science Facility Core (supported in part by NIH grant P30 ES01247) for assisting in set up of the novel object recognition test. Finally, the authors wish to thank Amy K. Huser for editorial assistance. This work was supported by NIH grants U19-AI067733 and U19-AI091036.

References

1. DiCarlo AL, Hatchett RJ, Kaminski JM, Ledney GD, Pellmar TC, Okunieff P, et al. Medical countermeasures for radiation combined injury: radiation with burn, blast, trauma and/or sepsis. [Report of an NIAID Workshop], March 26–27, 2007. Radiat Res. 2008; 169(6):712–21. [PubMed: 18494548]
2. Pellmar TC, Ledney GD. Combined Injury- Radiation in Combination with trauma, Infectious Disease, or chemical exposure. NATO RTG. 2005
3. Manthous CA, Jackson WL Jr. The 9–11 Commission's invitation to imagine: a pathophysiology-based approach to critical care of nuclear explosion victims Crit Care Med. 2007; 35(3):716–23.
4. Alpen EL, Sheline GE. The combined effects of thermal burns and whole body x irradiation on survival time and mortality. Ann Surg. 1954; 140(1):113–8. [PubMed: 13159151]
5. Brooks JW, Evans EI, Ham WT Jr. Reid JD. The influence of external body radiation on mortality from thermal burns. Ann Surg. 1952; 136(3):533–45. [PubMed: 14953182]
6. Moravan MJ, Olschowka JA, Williams JP, O'Banion MK. Cranial irradiation leads to acute and persistent neuroinflammation with delayed increases in T-cell infiltration and CD11c expression in C57BL/6 mouse brain. Radiat Res. 2011; 176(4):459–73. [PubMed: 21787181]
7. DiCarlo AL, Maher C, Hick JL, Hanfling D, Dainiak N, Chao N, et al. Radiation injury after a nuclear detonation: medical consequences and the need for scarce resources allocation. Disaster Med Public Health Prep. 2011; 5(Suppl 1):S32–44. [PubMed: 21402810]
8. Li J, Bentzen SM, Li J, Renschler M, Mehta MP. Relationship between neurocognitive function and quality of life after whole-brain radiotherapy in patients with brain metastasis. Int J Radiat Oncol Biol Phys. 2008; 71(1):64–70. [PubMed: 18406884]
9. Cherry JD, Liu B, Frost JL, Lemere CA, Williams JP, Olschowka JA, et al. Galactic cosmic radiation leads to cognitive impairment and increased abeta plaque accumulation in a mouse model of Alzheimer's disease. PloS one. 2012; 7(12):e53275. [PubMed: 23300905]

10. Gamache GL, Levinson DM, Reeves DL, Bidyuk PI, Brantley KK. Longitudinal neurocognitive assessments of Ukrainians exposed to ionizing radiation after the Chernobyl nuclear accident. Arch Clin Neuropsychol. 2005; 20(1):81–93. [PubMed: 15620815]
11. Mora AG, Ritenour AE, Wade CE, Holcomb JB, Blackbourne LH, Gaylord KM. Posttraumatic stress disorder in combat casualties with burns sustaining primary blast and concussive injuries. J Trauma. 2009; 66(4 Suppl):S178–85. [PubMed: 19359963]
12. Swann K, Berger J, Sprague S, Wu Y, Lai Q, Jimenez D, et al. Peripheral thermal injury causes blood–brain barrier dysfunction and matrix metalloproteinase (MMP) expression in rat. Brain Res. 2007; 1129(1):26–33. [PubMed: 17156757]
13. Gamelli RL, Liu H, He LK, Hofmann CA. Alterations of glucose transporter mRNA and protein levels in brain following thermal injury and sepsis in mice. Shock. 1994; 1(6):395–400. [PubMed: 7735967]
14. Evers LH, Bhavsar D, Mailander P. The biology of burn injury. Exp Dermatol. 2010; 19(9):777–83. [PubMed: 20629737]
15. Kallinen O, Maisniemi K, Bohling T, Tukiainen E, Koljonen V. Multiple organ failure as a cause of death in patients with severe burns. J Burn Care Res. 2012; 33(2):206–11. [PubMed: 21979843]
16. Schwacha MG. Macrophages and post-burn immune dysfunction. Burns. 2003; 29:1–14. [PubMed: 12543039]
17. Palmer JL, Deburghgraeve CR, Bird MD, Hauer-Jensen M, Kovacs EJ. Development of a combined radiation and burn injury model. J Burn Care Res. 2011; 32(2):317–23. [PubMed: 21233728]
18. Cheung MC, Spalding PB, Gutierrez JC, Balkan W, Namias N, Koniaris LG, et al. Body surface area prediction in normal, hypermuscular, and obese mice. J Surg Res. 2009; 153(2):326–31. [PubMed: 18952236]
19. Matousek SB, Ghosh S, Shaftel SS, Kyrkanides S, Olschowka JA, O'Banion MK. Chronic IL-1beta-mediated neuroinflammation mitigates amyloid pathology in a mouse model of Alzheimer's disease without inducing overt neurodegeneration. J Neuroimmune Pharmacol. 2012; 7(1):156–64. [PubMed: 22173340]
20. Dere E, Huston JP, De Souza Silva MA. The pharmacology, neuroanatomy and neurogenetics of one-trial object recognition in rodents. Neurosci Biobehav Rev. 2007; 31(5):673–704. [PubMed: 17368764]
21. Biffl WL, Moore EE, Moore FA, Peterson VM. Interleukin-6 in the injured patient. Marker of injury or mediator of inflammation? Ann Surg. 1996; 224(5):647–64. [PubMed: 8916880]
22. Ransohoff RM, Perry VH. Microglial physiology: unique stimuli, specialized responses. Annu Rev Immunol. 2009; 27:119–45. [PubMed: 19302036]
23. Lee S, Varvel NH, Konerth ME, Xu G, Cardona AE, Ransohoff RM, et al. CX3CR1 deficiency alters microglial activation and reduces beta-amyloid deposition in two Alzheimer's disease mouse models. Am J Pathol. 2010; 177(5):2549–62. [PubMed: 20864679]
24. Herber DL, Mercer M, Roth LM, Symmonds K, Maloney J, Wilson N, et al. Microglial activation is required for Abeta clearance after intracranial injection of lipopolysaccharide in APP transgenic mice. J Neuroimmune Pharmacol. 2007; 2(2):222–31. [PubMed: 18040847]
25. Norden DM, Godbout JP. Review: microglia of the aged brain: primed to be activated and resistant to regulation. Neuropathol Appl Neurobiol. 2013; 39(1):19–34. [PubMed: 23039106]
26. Montgomery SL, Bowers WJ. Tumor necrosis factor-alpha and the roles it plays in homeostatic and degenerative processes within the central nervous system. J Neuroimmune Pharmacol. 2012; 7(1):42–59. [PubMed: 21728035]
27. Wu MD, Hein AM, Moravan MJ, Shaftel SS, Olschowka JA, O'Banion MK. Adult murine hippocampal neurogenesis is inhibited by sustained IL-1beta and not rescued by voluntary running. Brain Behav Immun. 2012; 26(2):292–300. [PubMed: 21983279]
28. Hein AM, Stasko MR, Matousek SB, Scott-McKean JJ, Maier SF, Olschowka JA, et al. Sustained hippocampal IL-1beta overexpression impairs contextual and spatial memory in transgenic mice. Brain Behav Immun. 2010; 24(2):243–53. [PubMed: 19825412]

29. Brown JP, Couillard-Despres S, Cooper-Kuhn CM, Winkler J, Aigner L, Kuhn HG. Transient expression of doublecortin during adult neurogenesis. J Comp Neurol. 2003; 467(1):1–10. [PubMed: 14574675]
30. Fujita S, Kato H, Schull WJ. The LD50 associated with exposure to the atomic bombing of Hiroshima and Nagasaki. J Radiat Res. 1991; (32 Suppl):154–61. [PubMed: 1762100]
31. Johnston CJ, Manning C, Hernady E, Reed C, Thurston SW, Finkelstein JN, et al. Effect of total body irradiation on late lung effects: hidden dangers. Int J Radiat Biol. 2011; 87(8):902–13. [PubMed: 21574903]
32. Heinrich SA, Messingham KA, Gregory MS, Colantoni A, Ferreira AM, Dipietro LA, et al. Elevated monocyte chemoattractant protein-1 levels following thermal injury precede monocyte recruitment to the wound site and are controlled, in part, by tumor necrosis factor-alpha. Wound Repair Regen. 2003; 11(2):110–9. [PubMed: 12631298]
33. Coban YK, Aral M. Serum IL-18 is increased at early postburn period in moderately burned patients. Mediators Inflamm. 2006; 2006(2):16492. [PubMed: 16883062]
34. Jeschke MG, Gauglitz GG, Kulp GA, Finnerty CC, Williams FN, Kraft R, et al. Long-term persistance of the pathophysiologic response to severe burn injury. PloS one. 2011; 6(7):e21245. [PubMed: 21789167]
35. Lantos J, Foldi V, Roth E, Weber G, Bogar L, Csontos C. Burn trauma induces early HMGB1 release in patients: its correlation with cytokines. Shock. 2010; 33(6):562–7. [PubMed: 19997053]
36. Orman MA, Nguyen TT, Ierapetritou MG, Berthiaume F, Androulakis IP. Comparison of the cytokine and chemokine dynamics of the early inflammatory response in models of burn injury and infection. Cytokine. 2011; 55(3):362–71. [PubMed: 21652218]
37. Dantzer R, Bluthe RM, Gheusi G, Cremona S, Laye S, Parnet P, et al. Molecular basis of sickness behavior. Ann N Y Acad Sci. 1998; 856:132–8. [PubMed: 9917873]
38. Semmler A, Frisch C, Debeir T, Ramanathan M, Okulla T, Klockgether T, et al. Long-term cognitive impairment, neuronal loss and reduced cortical cholinergic innervation after recovery from sepsis in a rodent model. Exp Neurol. 2007; 204(2):733. [PubMed: 17306796]
39. Weberpals M, Hermes M, Hermann S, Kummer MP, Terwel D, Semmler A, et al. NOS2 gene deficiency protects from sepsis-induced long-term cognitive deficits. J Neurosci. 2009; 29(45): 14177–84. [PubMed: 19906966]
40. Orman MA, Ierapetritou MG, Berthiaume F, Androulakis IP. Long-term dynamic profiling of inflammatory mediators in double-hit burn and sepsis animal models. Cytokine. 2012; 58(2):307–15. [PubMed: 22402033]
41. Plackett TP, Gamelli RL, Kovacs EJ. Gender-based differences in cytokine production after burn injury: a role of interleukin-6. J Am Coll Surg. 2010; 210(1):73–8. [PubMed: 20123335]
42. Monje ML, Toda H, Palmer TD. Inflammatory blockade restores adult hippocampal neurogenesis. Science. 2003; 302(5651):1760–5. [PubMed: 14615545]
43. Villeda SA, Luo J, Mosher KI, Zou B, Britschgi M, Bieri G, et al. The ageing systemic milieu negatively regulates neurogenesis and cognitive function. Nature. 2011; 477(7362):90–4. [PubMed: 21886162]
44. Clark RE, Zola SM, Squire LR. Impaired recognition memory in rats after damage to the hippocampus. J Neurosci. 2000; 20(23):8853–60. [PubMed: 11102494]
45. Hammond RS, Tull LE, Stackman RW. On the delay-dependent involvement of the hippocampus in object recognition memory. Neurobiol Learn Mem. 2004; 82(1):26–34. [PubMed: 15183168]
46. Gordon PH, Moore DH, Miller RG, Florence JM, Verheijde JL, Doorish C, et al. Efficacy of minocycline in patients with amyotrophic lateral sclerosis: a phase III randomised trial. Lancet Neurol. 2007; 6(12):1045–53. [PubMed: 17980667]
47. Investigators NN-P. A pilot clinical trial of creatine and minocycline in early Parkinson disease: 18-month results. Clin Neuropharmacol. 2008; 31(3):141–50. [PubMed: 18520981]

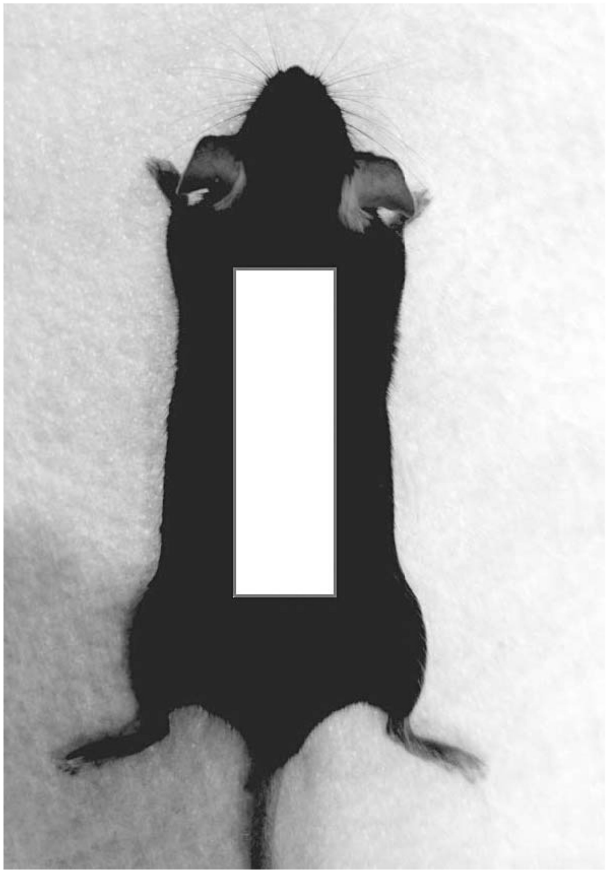

FIG. 1.
Depiction of approximate mouse body area exposed for 10% thermal injury. Boxed area represents the approximate area exposed to heated water during thermal injury. Great care was taken to not expose the neck, limbs or tail.

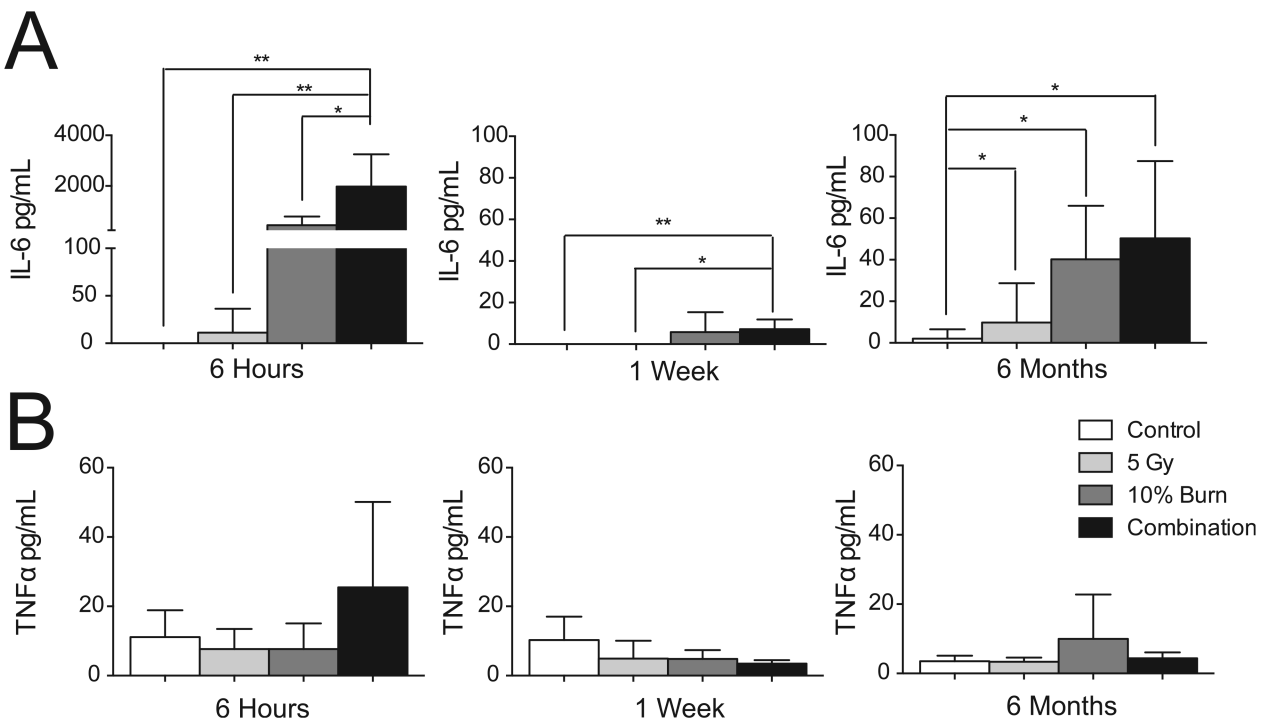

FIG. 2.

Plasma levels of IL-6 and TNF-α. ELISA analysis for IL-6 (panel A) and TNF-α (panel B) levels at 6 h, 1 week and 6 months post-injuries. Data was analyzed with a Kruskal-Wallis test. Data is displayed as mean ± SD, n = 5−9 animals per time point. **P* < 0.05, ***P* < 0.01.

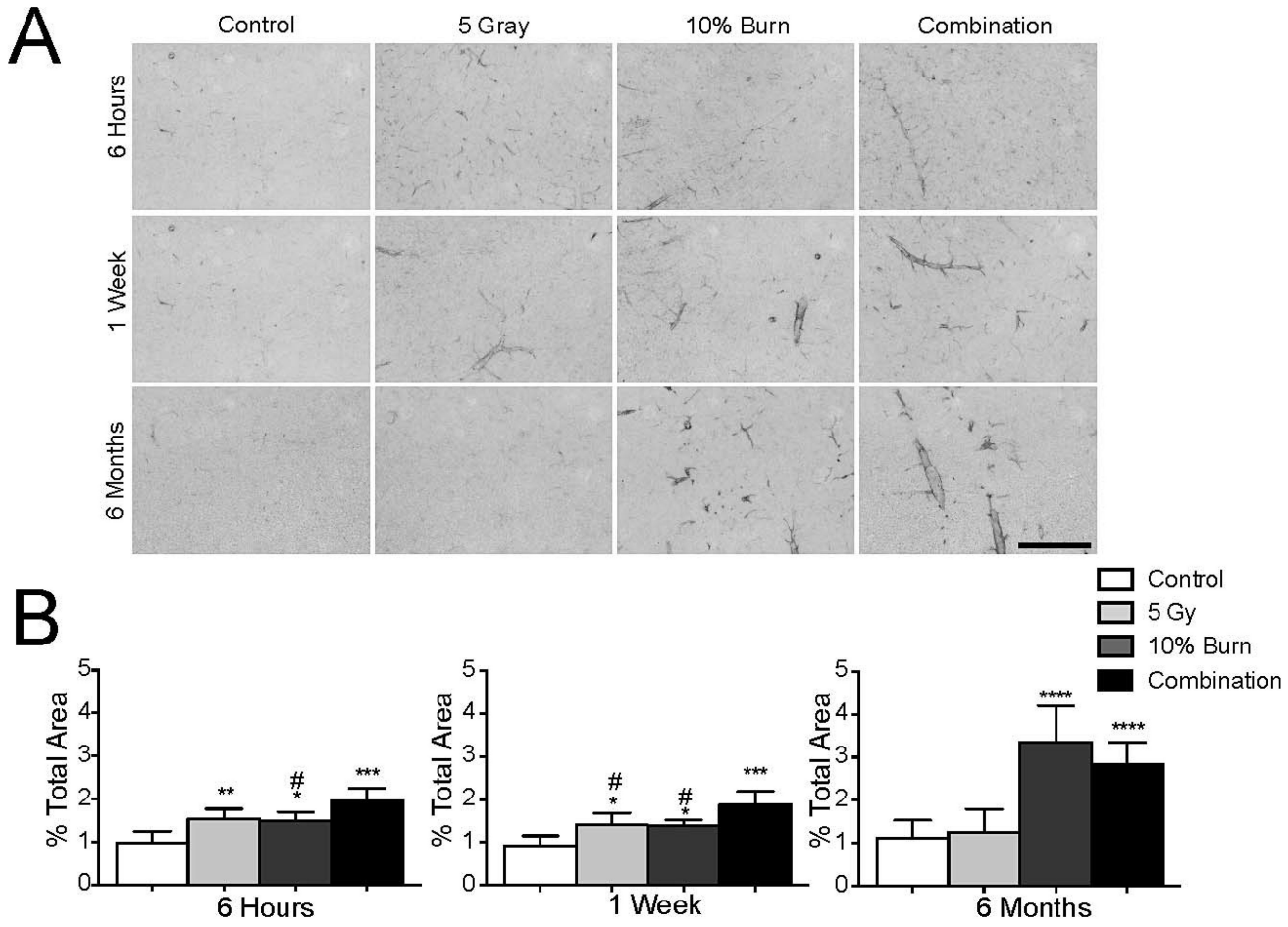

FIG. 3.

Injury leads to vascular activation. Panel A: Representative images of ICAM-1 staining. Scale bar represents 100 μm. Panel B: ICAM-1 area was measured as a percentage of total area in the entire cortex in 3 serial sections with the results being averaged together. Results were analyzed with a one-way ANOVA and a Bonferroni post-test. Data is displayed as mean ± SD, n = 5−10. *Denotes comparison to control and #denotes comparison to combined injury. *$P < 0.05$, **$P < 0.01$, ***$P < 0.001$, ****$P < 0.0001$, #$P < 0.05$.

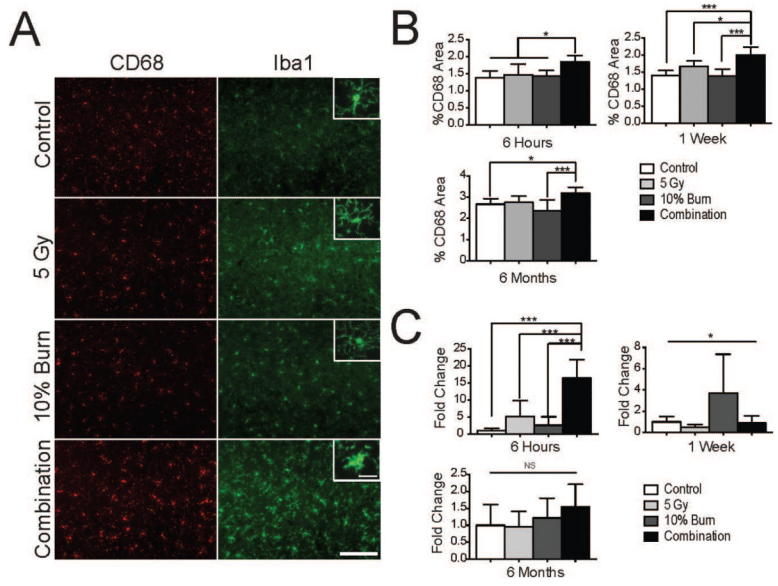

FIG. 4.

Combined injury synergistically upregulates glial activation. Panel A: Representative images of CD68 and Iba1 staining at 6 h. Scale bar indicates 100 μm. Inset scale bar indicates 20 μm. Panel B: CD68 area was measured as percentage total area in the cortex using two images from each of 3 hippocampal sections per subject (6 total fields per animal) with the results being averaged together. Panel C: qRT-PCR analysis of TNF-α mRNA levels from half brain lysates. Please note that the y-axis scale changes for each time point. Data was analyzed with a one-way ANOVA and a Bonferroni post-test. Data displayed as mean ± SD, n = 5−10 animals per time point. **P* < 0.05, ****P* < 0.001.

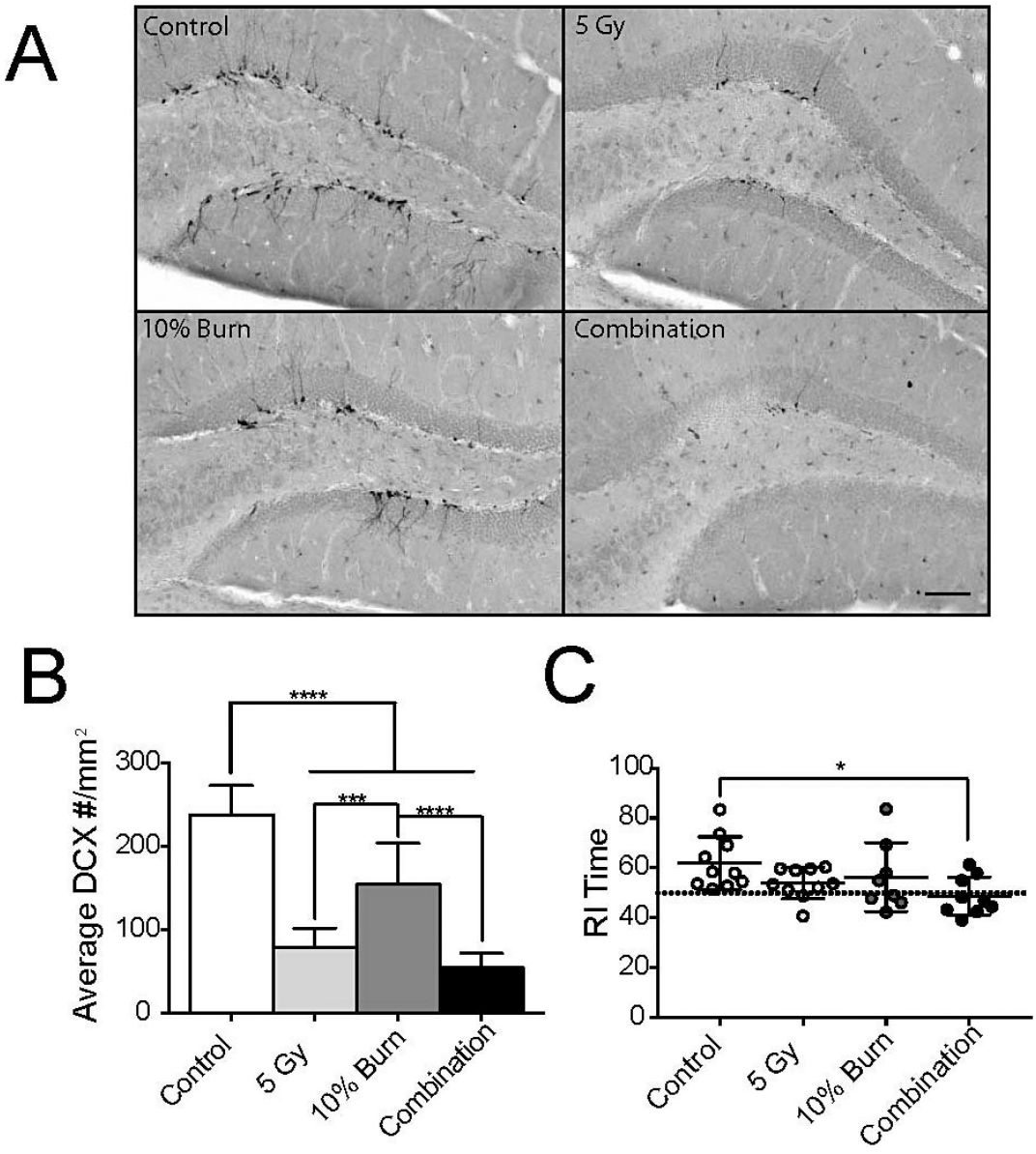

FIG. 5.

Combined injury results in impaired neurogenesis and cognition. Panel A: Representative images of doublecortin+ cells in the dentate gyrus at 6 months. Scale bar indicated 150 μm. Panel B: Average number of doublecortin+ cells per mm^2. Panel C: Novel object recognition test using the recognition index (RI) generated for time spent with the novel object. Dashed line indicates no object preference. Each dot represents a single animal. Data was analyzed with a one-way ANOVA and a Bonferroni post-test. Data displayed as mean ± SD, n = 5−10 animal per time point. *$P < 0.05$, ***$P < 0.001$, ****$P < 0.0001$.